CIRP Annals - Manufacturing Technology 66 (2017) 495–498

Contents lists available at ScienceDirect

CIRP Annals - Manufacturing Technology

journal homepage: http://ees.elsevier.com/cirp/default.asp

Uncertainty evaluation of indentation modulus in the nano-range: Contact stiffness contribution

Giulio Barbato [a], Gianfranco Genta [a], Roberto Cagliero [b], Maurizio Galetto [a], Matthew J. Klopfstein [c], Don A. Lucca (1)[c], Raffaello Levi (1)[a,*]

[a] Department of Management and Production Engineering, Politecnico di Torino, Corso Duca degli Abruzzi 24, 10129 Torino, Italy
[b] Department of Applied Science and Technology, Politecnico di Torino, Corso Duca degli Abruzzi 24, 10129 Torino, Italy
[c] School of Mechanical and Aerospace Engineering, Oklahoma State University, 218 Engineering North, Stillwater, OK 74078, USA

ARTICLE INFO

Article history:
Available online 28 April 2017

Keywords:
Nano indentation
Uncertainty
Methodology

ABSTRACT

Evaluation of indentation modulus by instrumented indentation in the nano-range can use one of two methods for contact stiffness evaluation, according to current ISO standards. The relevance of contact stiffness, suggested by a preliminary uncertainty analysis, prompted development of improved evaluation procedures. Data on a series of indentation tests, performed in an international comparison on tungsten and fused silica with forces in the millinewton range, were analysed with standard methods, and two alternative ones. Uncertainty evaluation revealed some shortcomings in the standard methods concerning the estimation of contact stiffness and indentation modulus; some definite advantages are shown with improved procedures.

© 2017 CIRP. Published by Elsevier Ltd. All rights reserved.

1. Introduction

Evaluation of the elastic modulus by instrumented indentation involves complex stress–strain fields, requiring algorithms which consider several factors in addition to force and displacement, such as instrument compliance and the effects of material sink-in or pile-up [1]. Ranking the main factors in terms of their contributions to uncertainty may be achieved by a systematic analysis, according to established guidelines [2]. In the case at hand, a preliminary investigation identified contact stiffness *S*, the slope of the tangent line at the start of the unloading phase (see Fig. 1), as an important factor contributing to uncertainty in the nano hardness range.

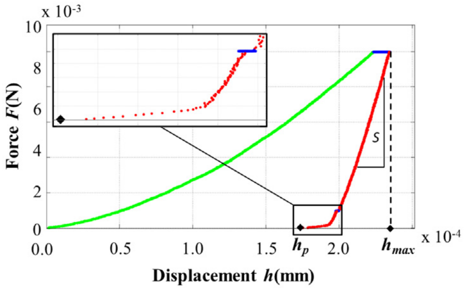

Fig. 1. Experimental indentation curve of force *F* vs. displacement *h*, with a detail of the zone near complete unloading, pertaining to a test on tungsten with a Berkovich indenter at 10 mN maximum force.

Evaluation of such a factor is awkward, as significant differences are often observed between results obtained according to the mathematical models covered by ISO 14577 [3]. The first, a linear model [4], fits the experimental data to a first approximation only, yielding substantially biased estimates. A closer fit is provided by the second, a power law model [5], whose weak point concerns inclusion of the residual indentation depth h_p at zero load. The corresponding experimental point is ill-defined, being affected by typical zero level scatter, and identified by the intersection of two lines forming a very small angle; furthermore, because of the relatively large distance from the region where the slope is to be estimated, small changes in h_p can result in large changes in *S*.

No model appears to outperform the other, as the linear model, although biased towards lower values of *S*, leads to results usually more repeatable than the power law model. Bias may be less objectionable than scatter, since, owing to a complex displacement pattern (see Fig. 2), material properties estimated from hardness measurements are related, but not necessarily equal to those obtained by conventional methods, for example tensile tests.

A critical aspect concerns the portion of experimental data used for estimation of the slope at the beginning of the unloading curve. With the first model, the smaller the range the lower the deviations from the linear form, however also, the larger the uncertainty of the estimated slope. While an optimum value of the portion used may be defined according to, for example, a procedure described elsewhere [6], in the case at hand, ranges specified by ISO 14577 were adhered to for reference purposes.

In light of these shortcomings, two further models were examined, with an initial linear trend morphing into a curved part [7,8]. The use of these methods in the analysis of experimental data

* Corresponding author.
E-mail address: raffaello.levi@polito.it (R. Levi).

http://dx.doi.org/10.1016/j.cirp.2017.04.060
0007-8506/© 2017 CIRP. Published by Elsevier Ltd. All rights reserved.

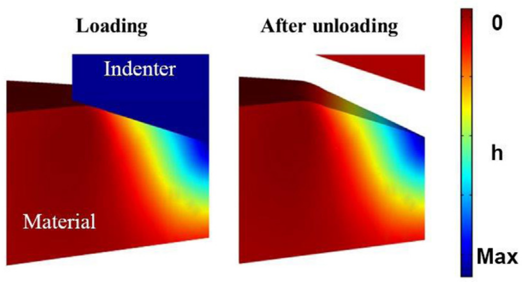

Fig. 2. Schematic cross section of an indentation, showing a typical computed vertical displacement pattern.

obtained from tests on reference materials (tungsten and fused silica) [9] showed potential improvements in terms of the consistency of the results.

2. Methods for contact stiffness evaluation

2.1. Standard methods

ISO 14577 covers two methods for evaluating the contact stiffness $S = (\partial F/\partial h)|_{h_{max}}$.

The linear extrapolation method (LE) assumes the first portion of the unloading curve is linear [4]. The model is identified by linear regression, with the slope equal to the contact stiffness S.

The power law method (PL) describes the bulk of the unloading curve as

$$F = B \cdot (h - h_p)^m \qquad (1)$$

where the terms B and m are estimated by least squares fitting to the experimental data within an interval usually between 98% and 20% of F_{max}. The range may be modified according to the 'quality' of the unloading curve, down to 50% of F_{max}. The slope at h_{max} is $S = B \cdot m \cdot (h_{max} - h_p)^{m-1}$.

ISO 14577 uses h_p, corresponding to the residual indentation depth at full unloading, as a fixed point. In the original paper describing PL [10], h_p is considered a parameter of a nonlinear regression, somehow mitigating the disturbing effects of a fixed point, with a high uncertainty and a location far from the region of interest. Empirical extrapolation of the unloading curve is used to estimate h_p, since otherwise convergence of the algorithms may not be taken for granted, owing to the scatter near complete unloading, shown for example, in the inset of Fig. 1.

2.2. Alternative methods

Two mathematical models addressing some of the shortcomings of the aforementioned methods were considered, with a nearly linear initial trend followed by a path with increasing curvature, the first sinusoidal (SN), and the second logarithmic (LN) [7,8]. Taking an 80% range of the unloading curve, both models fit experimental data reasonably well. Resorting to an appropriate reference system and scaling the h and F coordinates, with $X = k_x \cdot (h_{max} - h)$ and $Y = k_y \cdot (F_{max} - F)$, the first model can be written as

$$F = F_{max} - \frac{\sin[k_x \cdot (h_{max} - h)]}{k_y} \qquad (2)$$

and the second as

$$F = F_{max} - \frac{\ln[k_x \cdot (h_{max} - h) + 1]}{k_y} \qquad (3)$$

In either case the fitting parameters k_x and k_y are identified by nonlinear regression, enabling estimation and uncertainty evaluation of $S = k_x/k_y$. Which model fits experimental data best depends mainly upon the elasto-plastic properties of the material.

3. Analysis of indentation unloading curves

3.1. Experimental data

A comprehensive set of data was analysed, drawn from tests performed at Oklahoma State University within the framework of a CIRP sponsored international comparison on nanoindentation. Two reference materials were considered, tungsten and fused silica, with adequate sample homogeneity being confirmed by long industrial experience [9]. Experiments performed with a Berkovich indenter at four maximum force levels ranging between 0.5 mN and 10 mN were considered, indentation depths being typically within the nano-range.

3.2. Contact stiffness evaluation

In the linear extrapolation (LE), sine (SN) and logarithmic (LN) cases, contact stiffness S is a parameter of the regression of F on h, and evaluation of the corresponding uncertainty is straightforward. In the power law (PL) case, given the model in Eq. (1), the law of propagation of uncertainty [2] is exploited. The methods were compared by considering uncertainty intervals at 95% confidence level of the measured contact stiffness S_m for the case of a maximum force of 10 mN for both fused silica and tungsten. PL was considered with ranges of about 50%, 65% and 80% of the unloading curve (see Fig. 3).

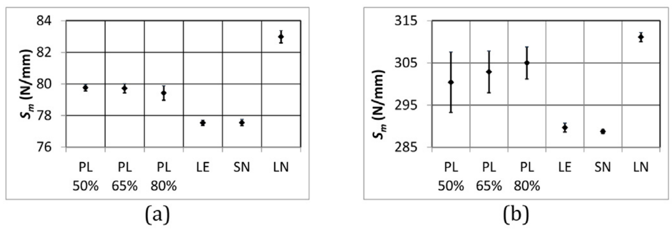

Fig. 3. Uncertainty intervals (95% confidence level) of the measured contact stiffness S_m according to four methods at 10 mN for fused silica (a) and tungsten (b). PL was considered with a range of about 50%, 65% and 80% of the unloading curve.

For the case of a maximum force of 10 mN, for both fused silica and tungsten, LE and SN values are rather close, while LN and PL values tend to exceed the former two. Uncertainty intervals pertaining to PL tend to exceed the others, more so for tungsten. Similar considerations hold for the other conditions of maximum force. In order to compare the methods, the regression residuals pattern should also be considered. An indentation curve for tungsten with a maximum force of 10 mN was taken as representative. Fig. 4 shows that residuals pertaining to LE have a marginal curvature (confirming that the method identifies a

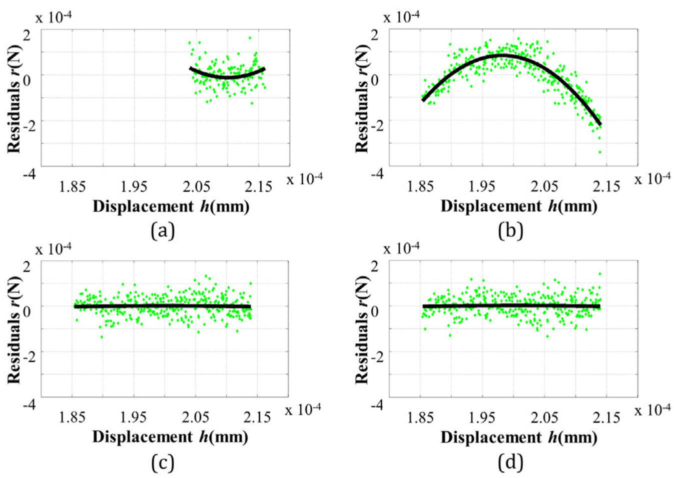

Fig. 4. Residuals plots pertaining to LE (a), PL with a range of about 80% (b), SN (c) and LN (d) at 10 mN indentation force for the case of tungsten.

secant line). The PL method exhibits a marked curvature (due to forcing the regression line to pass through the point h_p), while residuals appear random for both SN and LN.

4. Uncertainty evaluation of indentation modulus

Process measurement analysis in light of expected uncertainty can be performed according to GUM [2], in terms of a comprehensive mathematical model covering the steps described in ISO 14577 [3]. The main factors involved in the evaluation of the indentation modulus E_{IT} include Poisson ratios ν_s and ν_i of the material and diamond indenter respectively, as well as Young's modulus E_i of diamond, contact stiffness S and projected contact area of the indenter A_p, i.e.,

$$E_{IT} = (1-\upsilon_s^2)\cdot\left(\frac{2\cdot\sqrt{A_p}}{S\cdot\sqrt{\pi}} - \frac{1-\upsilon_i^2}{E_i}\right)^{-1} \tag{4}$$

Nominal values and related uncertainties of ν_s, ν_i and E_i may be obtained from the literature, while S and A_p depend on the force F and corresponding displacement h of the indenter into the tested material, evaluated close to the maximum indentation depth h_{max}. The measured values of indentation depth h_m, however, may have a zero offset h_0 (assuming a range of ten times its measurement resolution) and include a component due to the frame compliance C_f (constant to a first approximation), to be deducted in order to get an unbiased estimate of h, namely $h = h_m - h_0 - C_f{\cdot}F$. For the nanoindenter used, the compliance was $C_f = 0.4$ nm/mN with an expanded uncertainty of about 0.2 nm/mN.

Random errors affecting h_m, covering reproducibility, may be estimated in terms of scatter under the maximum applied force. Drift was accounted for by assuming a linear trend and applying regression accordingly, thus obtaining an expanded uncertainty of about 0.3 nm. Force was dealt with correspondingly, obtaining an expanded uncertainty of about 50 nN. The resolutions of the displacement and force sensors correspond to negligible contributions to the uncertainty of indentation modulus.

Since comparison of the performances of different methods of the evaluation of S is the aim, and the results are obtained from the same instrument, evaluation of systematic errors has a minor role in the case at hand.

The uncertainties of h_m and F are propagated over S and A_p. Taking for expediency, the reciprocal value of contact stiffness S, we can write:

$$\frac{1}{S} = \left(\frac{\partial h}{\partial F}\right)|_{h_{\max}} = \left(\frac{\partial h_m}{\partial F}\right)|_{h_{\max}} - C_f = \frac{1}{S_m} - C_f \tag{5}$$

The uncertainty of S is linked to the experimental data through the uncertainties $U(1/S_m)$, and $U(C_f)$, however both the value and variability of S_m depend on the model adopted to describe the unloading phase. Uncertainty is conveniently assessed also in terms of measurement replication, thus taking into account the relevant random errors.

The evaluation of the uncertainty contribution pertaining to the contact area A_p is affected by the departure from the nominal geometry of the actual indenter. Therefore for micro and nano hardness measurements the area function $A_p(h_g)$ is used, which gives the projected area as a function of geometrical distance h_g from the vertex [10]. For the case at hand, the indenter calibration yielded an area function approximated as

$$A_p = a_2\cdot h_g^2 + a_1\cdot h_g + a_0 \tag{6}$$

where the coefficients with corresponding expanded uncertainties are $a_0 = (-4.6 \pm 2.6)\times 10^3$ nm^2, $a_1 = (1.22 \pm 0.08)\times 10^3$ nm and $a_2 = 20.4 \pm 0.4$.

In order to estimate the projected area during indentation, depth h_g in Eq. (6) is substituted by h_c, the depth of the indentation where contact between indenter and material actually occurs, differing from h whenever sink-in or pile-up take place. When the depth of the contact zone is affected by sink-in a correction term is required [3], i.e.,

$$h_{c,\max} = h_{\max} - \varepsilon\cdot\frac{F_{\max}}{S} = h_{m,\max} - h_0 - \left[C_f + \varepsilon\cdot\left(\frac{1}{S_m} - C_f\right)\right]\cdot F_{\max} \tag{7}$$

with $\varepsilon = 0.75$ for pyramid shaped indenters. For uncertainty evaluation an extrinsic function of h, F, ε (considered as exact), C_f and S_m should be substituted into A_p, namely:

$$\begin{aligned} A_{p,\max} = {} & a_2\cdot\left\{h_{m,\max} - h_0 - \left[C_f + \varepsilon\cdot\left(\frac{1}{S_m} - C_f\right)\right]\cdot F_{\max}\right\}^2 \\ & + a_1\cdot\left\{h_{m,\max} - h_0 - \left[C_f + \varepsilon\cdot\left(\frac{1}{S_m} - C_f\right)\right]\cdot F_{\max}\right\} + a_0 \end{aligned} \tag{8}$$

which in turn is substituted into Eq. (4) to get the extrinsic mathematical model for the uncertainty evaluation of the indentation modulus E_{IT}. An example of an uncertainty budget [2] of E_{IT} for the case of the estimation of S with PL is shown in Table 1. The main contribution is due to the measured contact stiffness S_m followed by frame compliance C_f, other terms being much smaller.

A typical set of estimates of the indentation modulus of tungsten with relevant uncertainty intervals is shown in Fig. 5, depicting the effect of different methods for estimation of S. While LE and SN appear fully compatible, some systematic differences may be observed. Uncertainty for PL exceeds other values.

Table 1
Uncertainty table (according to GUM [2]) of the indentation modulus E_{IT} of tungsten with a maximum force of 5 mN, for an estimation of contact stiffness S with PL with a range of 50%.

Variable x_j		Type A	Type B	$u^2(x_j)$	c_j	$u_j^2(E_{IT})$	Rank
Symbol	Value	U_j	a_j				
ν_s	2.89E−01		1.0E−03	3.3E−07	−1.8E+05	1.1E+04	8
ν_i	7.00E−02		2.0E−02	1.3E−04	0.0E+00	0.0E+00	11
E_i	1.14E+06		2.0E+04	1.3E+08	6.6E−13	5.7E−17	10
ε	7.50E−01			0.0E+00	3.6E+04	0.0E+00	11
C_f	4.00E−04	2.4E−04		1.4E−08	7.5E+07	7.9E+07	2
h_0	0.00E+00		5.0E−07	8.3E−14	1.8E+09	2.8E+05	5
a_2	2.04E+01	4.1E−01		4.3E−02	−4.9E+03	1.0E+06	4
a_1	1.22E−03	8.1E−05		1.6E−09	−3.7E+07	2.2E+06	3
a_0	−4.65E−09	2.6E−09		1.8E−18	−2.8E+11	1.4E+05	6
$h_{m,max}$	1.49E−04	3.0E−07		2.3E−14	−1.8E+09	7.8E+04	7
F_{max}	4.96E−03	5.0E−08		6.4E−16	6.2E+06	2.5E−02	9
S_m	2.29E+02	7.7E+00		1.5E+02	1.2E+03	2.3E+08	1
E_{IT}	2.87E+05	N/mm^2	Variance, $u^2(E_{IT})$			3.2E+08	
			Standard uncertainty, $u(E_{IT})$			1.8E+04	
			Confidence level			95%	
			Expanded uncertainty, $U(E_{IT})$			3.5E+04	N/mm^2
			Relative expanded uncertainty			12%	

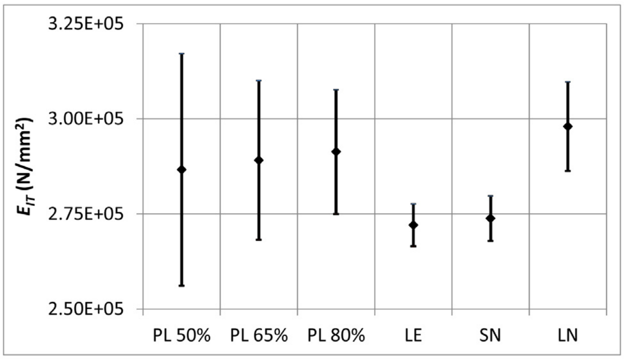

Fig. 5. Estimates of the indentation modulus of tungsten and relevant uncertainty intervals (95% confidence level) for a maximum force of 5 mN, for the different methods used for the estimation of S.

5. Discussion

Differences in measured contact stiffness S_m significantly influence the corresponding values of E_{IT}. In order to understand whether changes in S_m are significant, or masked by the effects of other factors, uncertainty contributions of the main factors are to be taken into account, in light of the type of application considered. In technical and scientific work, comparative tests are frequently performed on a given instrument and with a given indenter, for example, when assessing the effects of different technological treatments on materials. The reproducibility of the method is what is important in such a case, therefore the effects of C_f (which varies for different instruments), and of A_p (which varies for different indenters), may be almost negligible. Assuming that these effects do not exceed 20% of the uncertainties found by calibration, the relative contributions of the three main factors are shown in Fig. 6. When reproducibility is the important metrological characteristic, the effect of S_m appears to be the largest contributor except for the case of a maximum force of 10 mN, where the effect of C_f is seen to prevail for the LE, SN and LN methods.

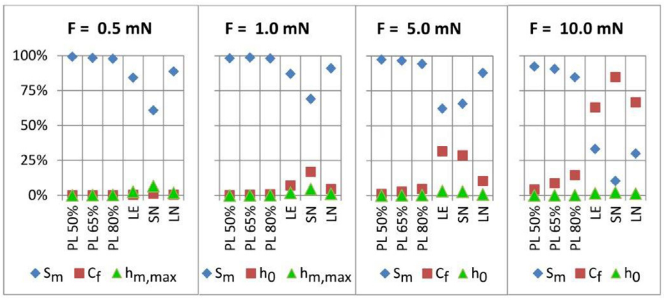

Fig. 6. Influence of the three main factors on uncertainty concerning E_{IT} reproducibility, shown on a percent basis for four indentation forces (see Section 4 for symbol definitions).

On the other hand, when comparison among tests performed with different instruments and/or different indenters is considered, the effect of calibration uncertainty on C_f is a major one, and to a minor extent also on A_p through a_1 and a_2, as shown in Fig. 7. S_m is then the main factor only for 0.5 mN, and to a minor extent for 1.0 mN. The effect of C_f prevails with LE, SN and LN at 5 mN. At 10 mN, C_f appears as the overwhelming factor and the effect of S_m may be neglected, but for the case of the PL method.

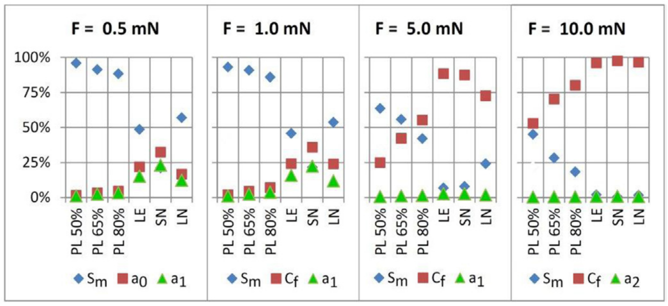

Fig. 7. Influence of the three main factors on E_{IT} overall uncertainty, shown on a percent basis for four indentation forces (see Section 4 for symbol definitions).

6. Conclusions

In light of the analysis of a comprehensive set of experimental data for nanoindentation tests, which were performed on tungsten and fused silica, some observations can be made. Methods currently covered by ISO 14577 for contact stiffness evaluation were found to exhibit some intrinsic shortcomings, in terms of, for example, bias owing to the disregard of the curvature of the unloading curve for the linear extrapolation method, and the residuals patterns showing unaccounted systematic effects which result from forcing an ill-defined point into the regression equation for the power law method. The alternative methods proposed show better agreement with experimental data, and lower scatter of estimates. A comprehensive mathematical model was developed in order to perform a systematic analysis of factors contributing to the uncertainty of indentation modulus estimation using GUM guidelines, enabling quantitative evaluation of the main contributions such as contact stiffness, frame compliance and indenter area function. Ranking of such contributions was made considering two different measurement tasks, one covering comparative tests performed on a given instrument with a given indenter, and another concerning, for example, round robin tests involving several different instruments and indenters. Contact stiffness was found to be a predominant factor in the first case, while for the second case, particularly at higher forces, frame compliance ranked among the main contributors.

References

[1] Lucca DA, Herrmann K, Klopfstein MJ (2010) Nanoindentation: Measuring Methods and Applications. *CIRP Annals — Manufacturing Technology* 59 (2):803–819.
[2] JCGM 100:2008, Evaluation of Measurement Data — Guide to the Expression of Uncertainty in Measurement (GUM), JCGM, Sèvres, France.
[3] ISO 14577:2015-6, Metallic Materials — Instrumented Indentation Test for Hardness and Materials Parameters, ISO, Geneva, Switzerland.
[4] Doerner MF, Nix WD (1986) A Method for Interpreting the Data from Depth-Sensing Indentation Instruments. *Journal of Materials Research* 1(4):601–609.
[5] Oliver WC, Pharr GM (2004) Measurement of Hardness and Elastic Modulus by Instrumented Indentation: Advances in Understanding and Refinements to Methodology. *Journal of Materials Research* 19(1):3–20.
[6] Barbato G, Bray A, Franceschini F, Romano D, Zompi A, Levi R (1998) An Automatic Procedure for Evaluation of Young's Modulus of Metallic Materials. *Journal of Testing and Evaluation* 26(1):64–69.
[7] Cagliero R, Barbato G, Maizza G, Genta G (2015) Measurement of Elastic Modulus by Instrumented Indentation in the Macro-Range: Uncertainty Evaluation. *International Journal of Mechanical Sciences* 101–102:161–169.
[8] Cagliero R (2016) *Instrumented Indentation Test in the Macro Hardness Range*, Lambert Academic Publishing, Saarbrücken, Germany.
[9] Herrmann K, Lucca DA, Klopfstein MJ, Menelao F (2010) CIRP Sponsored International Comparison on Nanoindentation. *Metrologia* 47(2):S50–S58.
[10] Oliver WC, Pharr GM (1992) An Improved Technique for Determining the Hardness and Elastic Modulus Using Load and Displacement Sensing Indentation Experiments. *Journal of Materials Research* 7(6):1564–1583.